

## Nonlinear Schrödinger-Equation Model of the Oscillating Two-Stream Instability\*

G. J. Morales, Y. C. Lee, and R. B. White†

*Physics Department, University of California, Los Angeles, California 90024*

(Received 10 December 1973)

This one-dimensional model exhibits a strong spatial collapse of the electric field when the self-consistent pump amplitude is held constant. The linear instability saturates if one allows for the self-consistent modification of the pump due to nonlinearities. The saturated state is characterized by relaxation oscillations and spatially localized electric fields of finite amplitude.

The linear theory<sup>1</sup> of the oscillating two-stream instability (OTSI) predicts that a large-amplitude electrostatic pump field whose frequency is slightly below the electron plasma frequency should cause the growth of nonoscillatory density perturbations. Investigations of this phenomenon are of relevance to studies of plasma heating, the laser-pellet problem, and the relativistic beam-plasma interaction. In addition, it is becoming increasingly evident in the literature<sup>2-6</sup> that the nonlinear evolution of the OTSI may play an important role in the final state of long-wavelength Langmuir turbulence. It is well known that under a wide variety of initial conditions, large amounts of plasma wave energy tend to concentrate in that region of the spectrum in which Landau damping is small (small wave numbers, large phase velocity). It has been found<sup>5</sup> that this spectral concentration of energy may induce a nonlinear instability (of the modulational type) that leads to the formation of spatially localized electric fields. Such a collapse process constitutes an efficient method of transferring energy to large wave numbers, where it is expected to be dissipated by wave-particle interactions.

In this Letter we present a specific example of the collapse process. It arises from a rather simplified model of the OTSI. The essence of this one-dimensional model consists of retaining the basic assumptions underlying the linear theory, such as the fluid description, neglect of ion inertial effects, and neglect of wave-particle interactions. The model contains several nonlinear effects, such as frequency shifts, harmonic generation, and pump modification.

The model equation can be obtained as follows.

$$2i\omega_0 \frac{\partial E}{\partial t} + 3\bar{v}_e^2 \frac{\partial^2 E}{\partial x^2} + \frac{\omega_p^2}{8\pi n_0 m c_s^2} (|E + E_0|^2 - |E + E_0|_{k=0}^2)(E + E_0) = S(t). \quad (4)$$

This is the model nonlinear Schrödinger equation. The time-dependent function  $S(t)$  arises mathematically from a simple spatial integration leading to Eq. (4). It represents physically the coupling be-

From the fluid equations for the electrons one obtains the expression

$$\frac{\partial^2 n_H}{\partial t^2} - 3\bar{v}_e^2 \frac{\partial^2 n_H}{\partial x^2} = \frac{e}{m} \frac{\partial}{\partial x} [(n_0 + n_L)E_H] \quad (1)$$

which relates the high- and low-density fluctuations,  $n_H$  and  $n_L$ , respectively, to the high-frequency electric field  $E_H$ . In Eq. (1)  $e$  and  $m$  are the electron charge and mass, respectively,  $\bar{v}_e$  is the electron thermal velocity, and  $n_0$  is the plasma density. Poisson's equation,

$$\frac{\partial(E_H - \tilde{E}_0)}{\partial x} = -4\pi e n_H, \quad (2)$$

connects  $n_H$  back to  $E_H$ . In Eq. (2)  $\tilde{E}_0$  represents the pump electric field generated by external charges. The motion of the ions is determined by

$$\frac{\partial v_L}{\partial t} = -\frac{\partial(\frac{1}{2}|v_H|^2)}{\partial x} - \frac{T_e + T_i}{Mn_0} \frac{\partial n_L}{\partial x}, \quad (3)$$

where  $v_L$  is the ion fluid velocity,  $T_e$  and  $T_i$  are the electron and ion temperature, respectively,  $M$  is the ion mass, and  $\frac{1}{2}|v_H|^2$  is the ponderomotive potential due to the high-frequency electric field. In the spirit of the linear theory of the OTSI one proceeds to neglect the ion inertial effects and thus obtains  $n_L/n_0 = -[M/(T_e + T_i)]|v_H|^2/2$ . With the definition

$$E_H = [E(x, t) + E_0] \exp(i\omega_0 t) + c.c.,$$

in which  $\omega_0$  is the pump frequency, one finds  $|v_H|^2 = (e/m\omega_0)^2 |E + E_0|^2$ . Combination of these relationships and definition of  $\omega_p$  and  $c_s$  as the electron plasma frequency and the ion sound speed, respectively, lead to

tween the external circuit and the plasma. To describe a particular experimental situation an additional equation (a circuit equation) for  $S(t)$  must be specified. A realistic problem would then consist of solving the coupled plasma and circuit equations self-consistently. The reason for subtracting the spatially homogeneous part ( $k=0$  component) of  $|E+E_0|$  in Eq. (4) is that such a term does not contribute to the effects of the ponderomotive force. In the limit in which  $|E| \ll E_0$  one can easily recover the linear theory of the OTSI from Eq. (4). The effects of electron collisions are included by setting  $\partial/\partial t \rightarrow \partial/\partial t + \nu_c$ , where  $\nu_c$  is the collision frequency. The model equation can be expressed in dimensionless form by using the following scaling:

$$E \rightarrow E/E_0, \quad t \rightarrow \omega_p t (E_0^2/16\pi n_0 m c_s^2) \equiv \Gamma t,$$

$$x \rightarrow k_D x (E_0^2/24\pi n_0 m c_s^2)^{1/2} \equiv k_0 x,$$

in which  $k_D = \omega_p \sqrt{\nu_e}$ . The only free parameter that appears in this scaled model is the value of  $\nu_c$ .

We have solved Eq. (4) numerically with the help of the on-line system at the University of California at Los Angeles. The numerical algorithm consists of decomposing Eq. (4) analytically into Fourier modes and evaluating the nonlinear term by the fast Fourier-transform method. The resulting coupled equations are then solved by integrating in time over the corresponding Green's functions. For the typical results presented in this Letter we used 32 Fourier modes. The length of the system can be adjusted so that the number of linearly unstable modes can be varied. Typically, this number ranges from one to nine modes. In solving Eq. (4) there are two extreme and highly idealized cases that can be isolated:

*Case A.*—In this case one legislates that  $S(t)$  is such that the spatially homogeneous part of  $E$  is equal to zero. This implies that the external circuit can overcome the nonlinear plasma loading so that the amplitude and phase of the self-consistent spatially homogeneous field are held constant.

*Case B.*—In this case one has the opposite idealized situation. It arises by legislating that  $S(t) = 0$ . This condition implies that the external circuit can not match the plasma loading because of the nonlinearities of Eq. (4). As a consequence, the amplitude and phase of the spatially homogeneous field within the plasma can be modified by the growth of the instability.

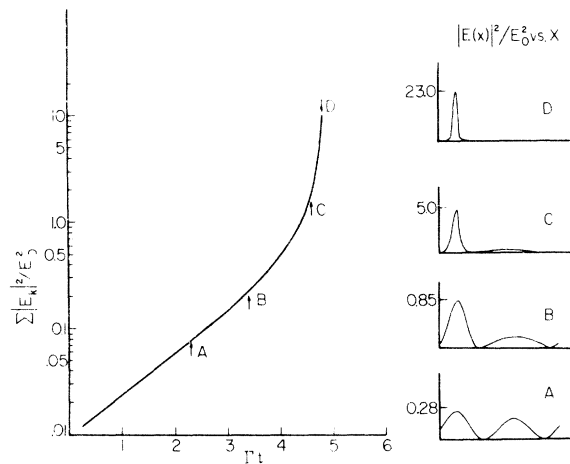


FIG. 1. Time evolution of total wave energy and corresponding spatial dependence of the electric field. Pump amplitude is constant.  $\nu_c/\Gamma = 0.5$ .

In Fig. 1 we present results characteristic of case A. The system is started by assigning small amplitudes to all modes and giving them random phases. The initial evolution is characterized by random amplitude and phase fluctuations. These fluctuations continue until the proper phase-matching conditions predicted by the linear theory of the OTSI are satisfied. At this stage the linearly unstable modes begin to exponentiate. The left-hand side of Fig. 1 shows the subsequent time evolution of the total wave energy. For early times the wave energy grows exponentially as predicted by linear theory. However, as the wave energy becomes comparable to the energy of the pump, a very strong nonlinear instability develops. To understand the behavior of the system it is helpful<sup>7</sup> to examine the spatial dependence of the electric field. This information is provided by the right-hand side of Fig. 1 for several key times in the evolution. At time A one observes a sinusoidal perturbation characteristic of early times. At time B the amplitude has grown and the spatial dependence exhibits a distortion arising from the interference with the nonlinearly generated second harmonic. At time C it is seen that the amplitude of the peak has grown rapidly and the electric field becomes localized in space. At time D we observe a clear example of spatial collapse of the electric field.

Figure 2 shows a typical Fourier spectrum observed at the collapse stage of the problem. The shape of the spectrum is given essentially by an exponential, as is characteristic of strong har-

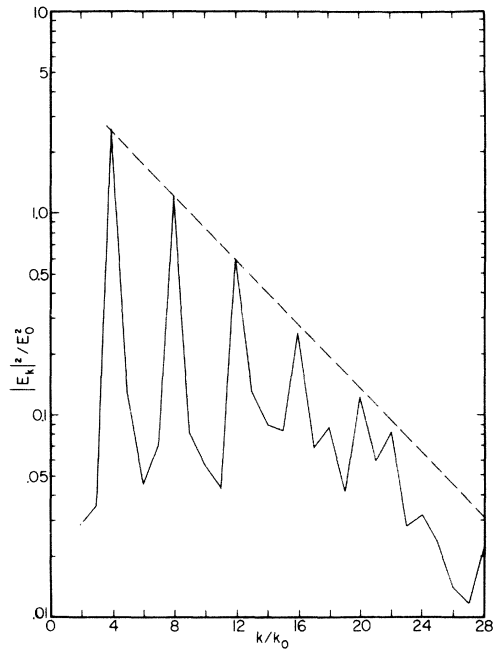


FIG. 2. Typical Fourier spectrum at the collapse stage. Fastest growing mode  $k/k_0=4$ .

monic generation by the fastest growing mode ( $k/k_0=4$  in this case). The strong nonlinear instability observed can be viewed as a type of self-modulation of the growth rate by the fastest growing mode. Keeping this dominant effect in Eq. (4) one can solve approximately for a spatially dependent growth rate. The expression one obtains indicates that the growth rate is enhanced near the peaks of  $|E|^2$  and decreases in the valleys; which particular peak gets enhanced depends on the initial phases. The reason why the spatial collapse is so rapid is that the modulation of the growth rate is a process that enters as an exponential of an exponential. Of course, in our simplified model there are no effects that can stop such a rapid collapse. It is expected that ion inertia and wave-particle interactions become very important at this stage of the problem and limit the amplitude of the localized electric fields. The results presented here are intended to illustrate that the collapse can take place within the confines of the physical effects contained in this model.

Figure 3 displays results corresponding to case B. The initialization of the system is as described previously for case A. It is observed in Fig. 3 that the wave energy grows exponentially and saturates, in contrast to case A. The

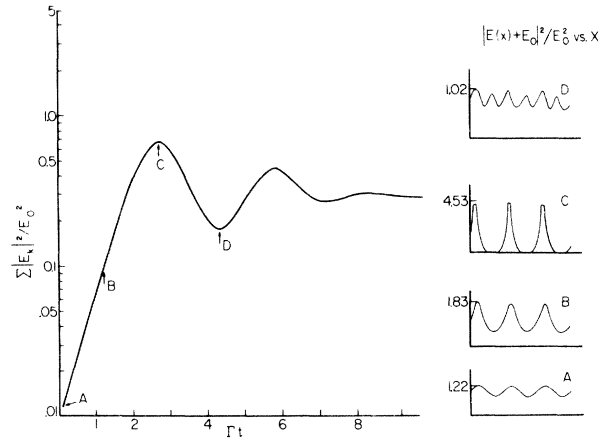


FIG. 3. Time evolution of total wave energy and corresponding spatial dependence of the electric field. Pump depletion is allowed.  $\nu_c/\Gamma=0.1$ .

right-hand side of Fig. 3 shows the spatial dependence of the quantity  $|E + E_0|^2/E_0^2$ . At time A a small-amplitude fluctuation is observed. At time B the fluctuation has grown and becomes slightly distorted. At time C one detects that spatially localized electric fields are also generated in this case. However, these structures do not experience a runaway collapse because the effective pump amplitude is reduced by the nonlinearities, which can generate a  $k=0$  component as well as harmonics. Instead of spatial collapse, in case B the system exhibits relaxation oscillations between the states exemplified by times C and D.

Another point of interest seen in Fig. 3 is that the wave energy at saturation can be smaller than the pump energy in some instances. The saturation level depends on how far above threshold is the initial pump amplitude (i.e., how small we make  $\nu_c/\Gamma$  in our model). In other runs we have made, it is observed that by decreasing  $\nu_c$  the saturation level approaches a value equal to 1 in the units used in Fig. 3.

In summary, a nonlinear Schrödinger-equation model of the oscillating two-stream instability exhibits a strong spatial collapse of the electric field when the self-consistent pump amplitude is held constant. The linear instability can be saturated if one allows for the self-consistent modification of the pump. The pump modification arises naturally from the nonlinearities of the model. In the saturated state there are two properties of experimental interest. One is the appearance of spatially localized electric

fields, the other is the relaxation oscillations. These distinct signatures may be helpful in identifying the oscillating two-stream instability. In a recent theoretical study<sup>6</sup> the existence of a random spectrum of localized electric fields has been invoked to explain the results of a computer simulation<sup>2</sup> of the OTSI. The nonlinear Schrödinger-equation model presented here gives a simple example of how certain localized electric fields can be formed during the nonlinear stages of the OTSI.

The authors wish to acknowledge helpful discussions with Professor K. Nishikawa and Dr. C. S. Liu.

\*Work partially supported by the U. S. Atomic Energy

Commission under Contract No. AT(4-03)-34, Project No. 157, and by the U. S. Office of Naval Research under Grant No. N00014-69-A-0200-4023.

†Permanent address: Institute for Advanced Study, Princeton, N. J. 08540.

<sup>1</sup>K. Nishikawa, *J. Phys. Soc. Jap* **24**, 916, 1152 (1968).

<sup>2</sup>J. J. Thomson, R. J. Faehl, and W. L. Kruer, *Phys. Rev. Lett.* **31**, 918 (1973).

<sup>3</sup>K. Nishikawa, Y. C. Lee, and C. S. Liu, *Bull. Amer. Phys. Soc.* **18**, 1366 (1973).

<sup>4</sup>L. I. Rudakov, *Dokl. Akad. Nauk SSSR* **207**, 821 (1972) [*Sov. Phys. Dokl.* **17**, 1166 (1973)].

<sup>5</sup>V. E. Zakharov, *Zh. Eksp. Teor. Fiz.* **62**, 1475 (1972) [*Sov. Phys. JETP* **35**, 908 (1972)].

<sup>6</sup>A. S. Kingsep, L. I. Rudakov, and R. N. Sudan, *Phys. Rev. Lett.* **31**, 1482 (1973).

<sup>7</sup>In strongly nonlinear systems the information obtained from the Fourier spectrum may not be very illustrative.

## Phase Transition in a Vertex Model in Three Dimensions

F. Y. Wu\*†

*Research School of Physical Sciences, The Australian National University,  
Canberra, Australian Capitol Territory 2600, Australia*

(Received 14 December 1973)

The exact transition temperature and the order of phase transition are determined for a vertex model in three dimensions. The transition is in general of first order with a latent heat and occurs in a limited region in the parameter space. Details of the region depend on the underlying lattice and differ significantly between lattices with high (fcc and bcc) and low (simple cubic and diamond) coordination numbers.

Investigation of phase transitions in lattice systems has centered around the study of vertex models. The most general result is that of the two-dimensional eight-vertex model<sup>1</sup> which includes the Ising and the ferroelectric models. Little is known, however, about the critical behavior of vertex models in three dimensions.<sup>2</sup>

In this Letter we report on some exact results for a three-dimensional vertex model. The analysis is an extension of our earlier discussion of a sixteen-vertex model.<sup>3</sup> In this earlier investigation, the fact that the model is two-dimensional is explicitly used. It turns out that, with slight modifications, the argument is also applicable to three-dimensional models. We can then determine, using only elementary considerations, the exact transition temperature and the nature of phase transition for a rather general vertex model in three dimensions. It is also noteworthy that a significant difference in the critical behavior is found between lattices with high and low coordi-

nation numbers.

Consider a lattice  $\mathcal{L}$  (in any dimensionality) of  $N$  vertices (or sites) with coordination number  $q$ . Assume cyclic boundary conditions and let the  $\frac{1}{2}qN$  edges of  $\mathcal{L}$  be independently covered by bonds. There are then  $2^{qN/2}$  distinct bond coverages on  $\mathcal{L}$ . Also at each vertex there are  $2^q$  different bond configurations. Associate a fixed energy to each of the  $2^q$  vertex configurations and let  $E$  be the sum of the  $N$  vertex energies for a given bond coverage,  $B$ , of  $\mathcal{L}$ . The partition for this " $2^q$ -vertex model" is then

$$Z = \sum_B e^{-E/kT} \quad (1)$$

The model we propose to consider has the following assignments for the vertex energy,  $E_v$ :

$$\begin{aligned} E_v &= n\epsilon \text{ for vertices having} \\ & n = 0, 1, \dots, q-1 \text{ bonds;} \\ & = a\epsilon \text{ for vertices having } q \text{ bonds.} \end{aligned} \quad (2)$$